Solar Phys (2014) 289:939–950
DOI 10.1007/s11207-013-0356-y

Radio Observation of Solar-Activity-Related mHz Oscillations

N.V. Hiep · P.T. Nhung · P. Darriulat · P.N. Diep · P.T. Anh · P.N. Dong · D.T. Hoai · N.T. Thao

Received: 14 February 2013 / Accepted: 3 July 2013 / Published online: 26 July 2013
© Springer Science+Business Media Dordrecht 2013

Abstract The VATLY radio telescope, operating at 1.415 GHz in Ha Noi, has been used to track the Sun in the summer – autumn months in 2012. Evidence has been obtained for solar activity, including occasional flares and variable oscillations with amplitudes at the percent level and periods of about 6 min. Comparison with data collected at the same frequency by the Learmonth Observatory in Australia suggests that the observed oscillations were associated with solar activity. A joint analysis of both data sets is presented, evaluating the correlations between them. We describe the common and different main features.

Keywords Corona: radio emission · Polarization: radio · Radio bursts: association with flares · Radio emission: active regions · Radio scintillation

1. Introduction

The VATLY radio telescope was used to track the Sun in the summer – autumn months in 2012. The details of the telescope were described in previous publications (Hiep *et al.* 2012, 2013), giving evidence for its good performance. Its antenna is a mobile parabolic dish, 2.6 m in diameter, remotely adjustable in elevation and azimuth, equipped with a receiver for frequencies in the region of the 21-cm hydrogen line. The feed includes a two-turn left polarization helix sensor, so that the telescope observes the right circular polarization component of the incoming wave.

A pointing accuracy of $\approx 0.3^\circ$ is obtained after applying pointing corrections of about one degree. The size of the beam (FWHM) was measured to be $5.5 \pm 0.3^\circ$.

The process of standard data collection consists of a sequence of successive measurements of 7.7 s duration each, digitizing data in the form of a frequency histogram covering approximately 1.2 MHz in 156 bins of 7.8 kHz width, obtained by stitching together three independent 500 MHz bandwidths. A super-heterodyne receiver (supplied from Custom Astronomical Support Services, Inc., Montana, USA) uses a local oscillator whose frequency

N.V. Hiep · P.T. Nhung · P. Darriulat (✉) · P.N. Diep · P.T. Anh · P.N. Dong · D.T. Hoai · N.T. Thao
VATLY/INST, 179 Hoang Quoc Viet, Cau Giay, Ha Noi, Vietnam
e-mail: darriulat@vinatom.gov.vn

range is 1370 – 1800 MHz and whose intermediate frequency is centred at 800 kHz with a 6 dB range of 0.5 – 3 MHz. The back end includes analog to digital conversion on a dedicated PCI card, and the data are transferred to a hard disk for off-line analysis. The typical system temperature is about 150 K.

Our study covers the period between mid-April and early September in 2012. During that time, the VATLY radio telescope was operated at a frequency of 1.415 GHz (slightly below the 21-cm hydrogen line) and was tracking the Sun. Our data were compared with data from the Learmonth Observatory taken at the same frequency during the same period.[1] Ha Noi and Learmonth are located at nearby longitudes (105.8°E and 114.1°E, respectively) and at nearly opposite latitudes (21.0°N and 22.2°S, respectively). The technical characteristics of the Learmonth radio telescope are essentially identical to those of the Ha Noi telescope, apart from the use of a linear instead of a helical sensor, implying detection of the linear and not the circular component of a wave. The observatory is staffed seven days a week from sunrise to sunset and contributes data to the US Air Force Weather Agency, to the US National Oceanic and Atmospheric Administration, and to the Global Oscillation Network Group. In addition to the 8-feet dish, it operates an 8.5-m dish (245 to 610 MHz), a 1-m dish (15.4 GHz), a swept frequency interferometric radiometer (30 to 80 MHz), and an optical telescope. Its long experience with solar measurements and its commitment to serve a large community make it a highly reliable source of data. From this joint analysis, we estimate that the noise level of the Learmonth radio telescope is lower than that of the Ha Noi telescope by a factor of about 1.7.

2. General Features

We observed the Sun nearly continuously starting on 18 April 2012. At the beginning of each morning session, a calibration run was taken; in some cases, a second run was taken early in the afternoon. Pointing corrections were evaluated and applied about every 30 min. Because they implied stopping the telescope movement, they caused an approximately 40 s pause in data taking. Another cause of such pauses was accidental (but rare) errors due to a poor contact on the signal cable.

The frequency spectra are well described by a linear form. The chi-square value (χ^2) of the best fit to such a form was used to eliminate some few spectra that contained too many poor measurements. The values taken in each spectrum by the mean power density and by the slope as a function of frequency were found to be Gaussian-distributed with relative σ values of 7.7 % and 6.8 %, respectively. The dependence on calendar time of the daily average of the power density is consistent with that measured at Learmonth and displays oscillations in phase with the $\approx$ 28-day rotation period of the Sun: maxima exceeded minima by 50 % and occurred around 10 June, 8 July, 5 August, and 2 September, giving evidence for an important longitudinal nonuniformity in solar activity (see Figure 7 below).

By comparing our data with the Learmonth data, we identified 30 flares common to both sets (Hiep, 2012). Nearly half of the identified flares are single flares with a typical duration of 1 – 2 min. Their radio signals usually rise more sharply than they decay. Most of the identified flares have typical amplitudes of about 15 %, with only three exceeding 40 %, of which one shows an increase by a factor of five. They are displayed in Figure 1 together with the corresponding Learmonth data. They occurred on 3, 6, and 10 July, after

[1] Australian Government, Bureau of Meteorology, Radio and Space Weather Services, http://www.ips.gov.au/World_Data_Centre/1/10.

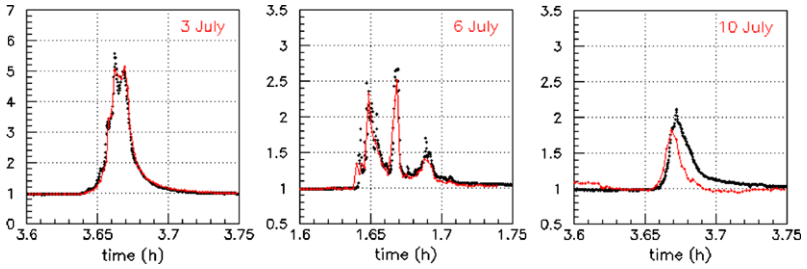

Figure 1 The three strongest flares as seen by the Learmonth Observatory (dots) and by the Ha Noi telescope (lines). The power density (ordinate) is normalized with respect to the pre-flare level. The time (abscissa) is in UT hours in the day.

Table 1 Comparison of GOES and Ha Noi flare data.

X-ray data (GOES)						Ha Noi (1.4 GHz)	
Name	Start	Peak	End	Class	Region	Peak	Max
gev_20120703_0336	03:36	03:42	03:48	C9.9	1515	03:40	×5.0
gev_20120706_0137	01:37	01:40	01:42	M2.9	1515	01:40	×2.5
gev_20120710_0337	03:36	03:42	03:48	C3.9	1520	03:41	×1.8

a particularly strong flare had erupted from a large active region (AR1515) on 6 July[2] just after we had turned off our radio telescope as the Sun was setting. While the first two show good agreement between Learmonth and Ha Noi data, the third flare was shorter in duration and its peak time was a few seconds earlier at Ha Noi. Table 1 compares our data with X-ray data from the *Geostationary Synchronous Environmental Satellite* (GOES).[3] The last of the three larger flares come from a different active region.

3. Oscillations: Observations

When zooming over the observed traces, one notes oscillations at the percent level, present in both Learmonth and Ha Noi data, with typical periods of 5 – 7 min. Figure 2 displays two such examples.

Telescope operation was interrupted not only during nights but also during weekends and on various other occasions. As a result, data-taking periods were disconnected and, during each of these, short interruptions sometimes occurred. To investigate the oscillation phenomenon, one must select time intervals that are long enough to contain several periods of the oscillation, yet short enough to be described by a single value of the period and not to display too complicated features. For this reason, we picked up data-taking periods lasting more than 25 min without interruptions of longer than 10 min. The periods longer than 53 min were split into shorter intervals. The average duration of individual time intervals is 40 min.

[2]NASA, http://www.nasa.gov/mission_pages/sunearth/news/News070712-X1.1flare.html.

[3]NOAA/NGDC, http://www.ngdc.noaa.gov/stp/solar/solarflares.html.

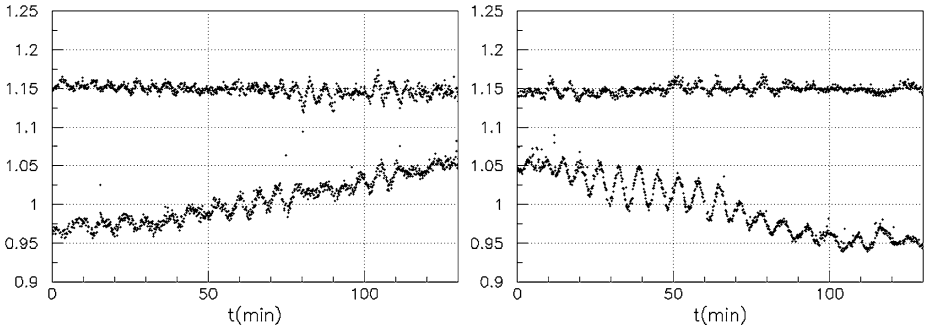

Figure 2 Two examples of oscillations simultaneously observed at Learmonth (upper traces) and Ha Noi (lower traces). Power densities are normalized to unity (the Learmonth data have been shifted up by 0.15 for clarity).

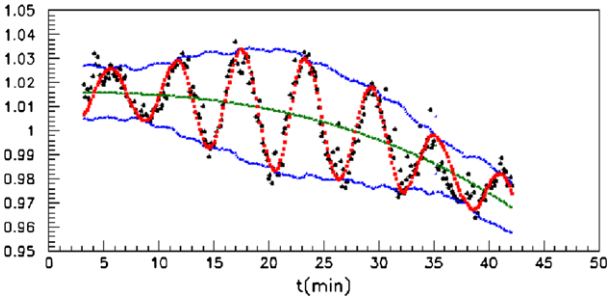

Figure 3 Fitting procedure: the data (dots) are first fitted by a cubic polynomial (central curve) over the whole interval. Their rms deviation from this polynomial, averaged over a 6-min sliding interval, defines the oscillation amplitude (outer curves), leaving two 3-min-wide dead regions at the edges of the time interval. In the last step, the period and phase of the oscillation are adjusted to minimize the χ^2 value (dotted curve).

In each time interval, the Ha Noi and Learmonth data were analysed separately, each being normalized to unity over the interval. The Learmonth data were taken every second, and we re-grouped them into larger time bins (≈ 8 s) that matched the Ha Noi measurements. The Ha Noi and Learmonth data sets were first fitted as a function of time t by a cubic polynomial $P(t)$. Figure 3 illustrates the procedure. The amplitude $A(t)$ of the observed oscillations is evaluated at each point as $\sqrt{2}$ times the root mean square deviation of the detected signal, $S(t)$, with respect to $P(t)$ in a 6-min sliding interval centred at the point. The data are then fitted by the form

$$S(t) = P(t) + A(t)\sin(2\pi t/T + \varphi). \tag{1}$$

A few bad data points or flares (0.3 % in total data points) were rejected on the basis of a too strong deviation with respect to the best-fit polynomial; then the polynomial fitting was repeated after data rejection. The fit of the sine wave requires good starting values of T and φ so that the χ^2 minimization process does not converge to a harmonic.

Each of the 304 time intervals considered in the analysis was carefully scrutinized and assigned to one of three possible categories depending on the adequacy of the form given by Equation (1) to describe the data.

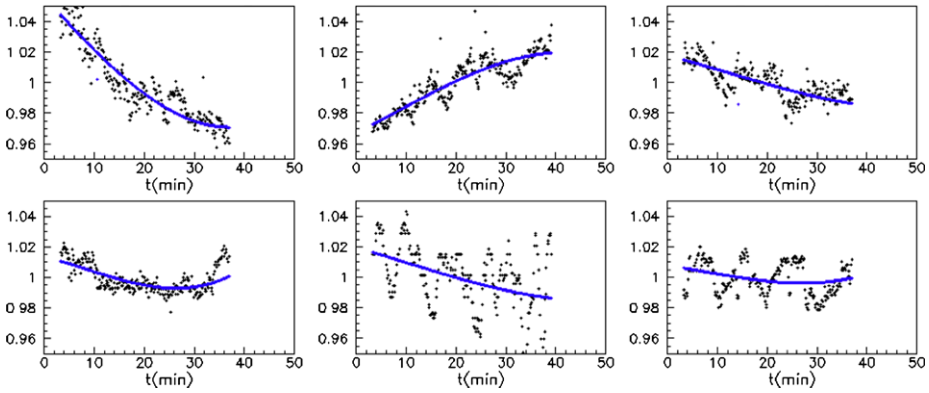

Figure 4 Three examples of category 0 intervals (Ha Noi data in the upper and Learmonth data in the lower panels). Examples without oscillation are seen together with examples of oscillations that cannot simply be described in terms of a single sine wave.

- We classified 109 intervals as category 0 if both the Ha Noi and Learmonth data sets were not properly described by Equation (1). Examples are displayed in Figure 4. They include cases without visible oscillation as well as cases with significant fluctuations that cannot be described using Equation (1).
- We classified 71 intervals as category 1 if only one of the Ha Noi and Learmonth data sets was properly described by Equation (1), but not the other. In 19 such intervals the Ha Noi data were properly described, in the remaining 52 intervals the Learmonth data were properly described. Examples are displayed in Figure 5.
- We classified 124 intervals as category 2 if both the Ha Noi and Learmonth data were properly described by Equation (1). Examples are given in Figure 6. The definition of "properly described" is somewhat arbitrary and cannot be easily quantified by simply using a threshold on the best-fit value of χ^2, for example. Some oscillations are very clear sine waves; others are sawtooth-like or quickly damped over the interval. This difficulty is kept in mind and taken into account below.

Figure 7 displays the distribution of the weekly number of intervals of each category over calendar time (in days) together with the daily-averaged solar flux measured at Learmonth (that measured at Ha Noi displays the same periodicity but is of poorer quality). The correlation between the occurrence of category 2 intervals and the phase of solar rotation suggests that they are favoured during the periods where solar radio emission is rising, namely when the more active hemisphere of the Sun is becoming visible from Earth; this is illustrated in the right panels of Figure 7 for the $3 \times 28 = 84$ day period from 28 May to 20 August 2012, which fully covers three periods of solar rotation. However, the observed distribution is only three standard deviations from uniform.

Figure 8 (left) shows the distribution of category 2 intervals in the $(\langle A_{\mathrm{L}}\rangle, \langle A_{\mathrm{H}}\rangle)$ plane, where A_{L} and A_{H} stand for the amplitudes measured at Learmonth and Ha Noi, respectively. Most intervals are confined to the wedge-shaped area $\frac{1}{4} < \langle A_{\mathrm{L}}\rangle / \langle A_{\mathrm{H}}\rangle < 1$. The mean values of $\langle A_{\mathrm{H}}\rangle$ and $\langle A_{\mathrm{L}}\rangle$ for these category 2 intervals are 1.68 % and 0.96 %, respectively, which are higher in the Ha Noi data than in the Learmonth data by a factor of 1.75. However, the two quantities were found to be uncorrelated.

Figure 8 (right) displays the distribution of category 2 intervals in the $(T_{\mathrm{L}}, T_{\mathrm{H}})$ plane where T_{L} and T_{H} are the Learmonth and Ha Noi periods, respectively. The figure suggests

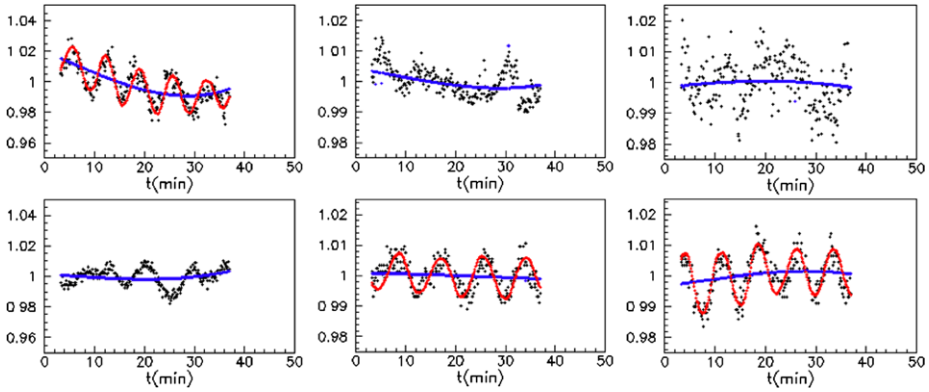

Figure 5 Three examples of category 1 intervals (Ha Noi data in the upper and Learmonth data in the lower panels). In each case, one of the data sets has been described by Equation (1) while the other could not be described with it. The curves show the cubic polynomial and sine wave best fits.

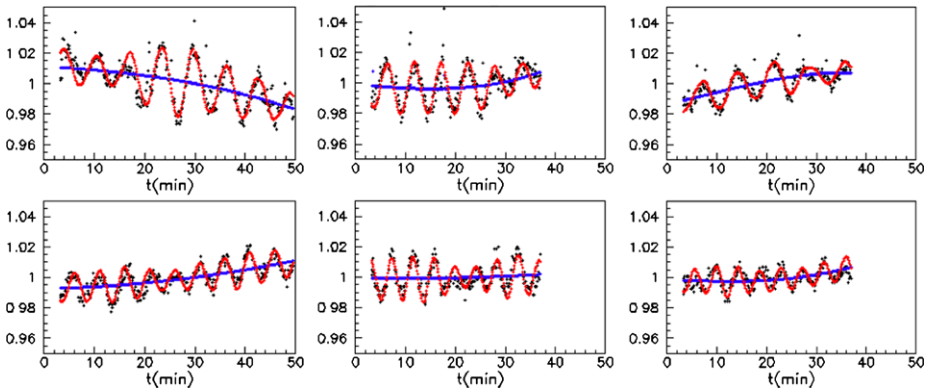

Figure 6 Three examples of category 2 intervals (Ha Noi data in the upper and Learmonth data in the lower panels). The curves show the cubic polynomial and sine wave best fits.

two distinct families of intervals separated by the line

$$T_{\mathrm{L}} = 2.2T_{\mathrm{H}} - 9.2 \text{ min}. \tag{2}$$

The family with T_{L} higher than this limit, defined here as family 1, is more populated (105 intervals) than family 2 (19 intervals). Family 1 displays a clear positive correlation of the form

$$T_{\mathrm{L}} = 2.2T_{\mathrm{H}} - 7.6 \text{ min}, \tag{3}$$

which we may rewrite as

$$T_{\mathrm{L}} - T_0 = k(T_{\mathrm{H}} - T_0), \tag{4}$$

with $T_0 = 6.3$ min and $k = 2.2$. While the oscillations observed at Learmonth and Ha Noi have similar periods on average, the spans that they cover differ significantly: if they were equal, the data would be distributed along the diagonal of Figure 8 (right). We have not

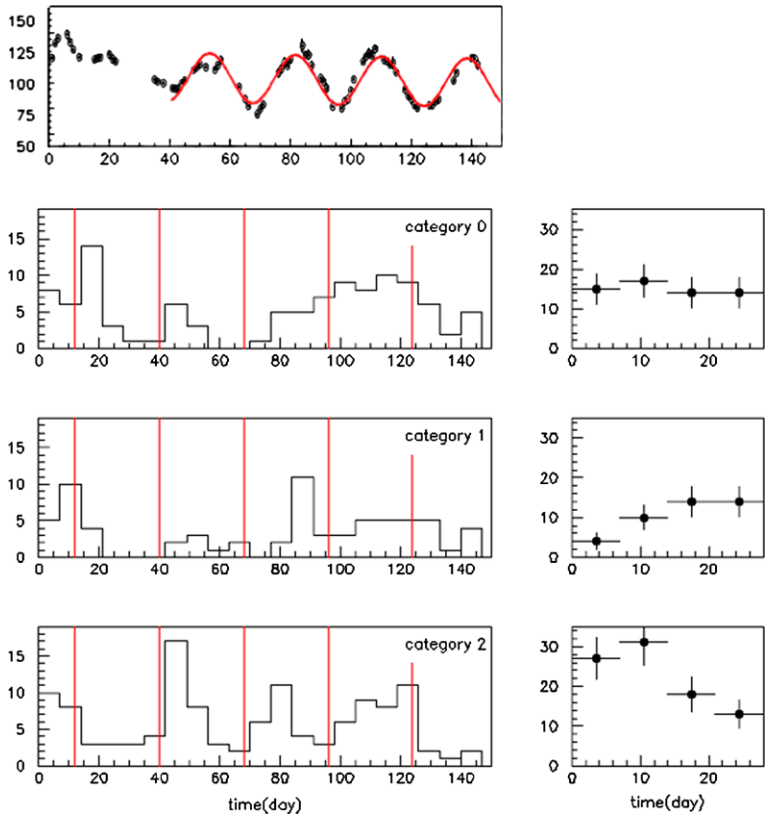

Figure 7 Upper left panel: Dependence on time (in days) of the daily average of the solar flux measured at Learmonth (in solar flux units). The red line is a sine wave fit starting on day 40 (28 May 2012). Lower left panels: Distribution of the weekly number of intervals of categories 0, 1, and 2 (from top to bottom) over calendar time, day 1 being 18 April 2012. The vertical lines indicate the minima of solar activity as shown in the upper panel. Right panel: Dependence on the phase of solar rotation of the number of intervals in each category (0 to 2 from top to bottom).

been able to identify other features that would clearly distinguish between families 1 and 2. The nominal uncertainty attached to the period measurement is exceedingly small, typically 2 – 3 s in the Ha Noi data and 1 – 2 s in the Learmonth data. However, the systematic uncertainty could be much larger and results mostly from the fact that the periods are not strictly constant over the intervals. To evaluate this effect, we split each interval into two halves and evaluated separately the periods T_1 and T_2 separately. They were measured in the first and second halves, respectively. Most of the spectra give an asymmetry

$$A = \left| \frac{T_1 - T_2}{T_1 + T_2} \right| \tag{5}$$

of the order of 6 % for Ha Noi and 5 % for Learmonth, but a tail at larger values of A brings these numbers to 10 % and 8 %, respectively. One should note that the smaller sizes of the half intervals are a trivial source of deterioration of the quality of the fits. We observed no correlation in A between the Ha Noi and Learmonth data and there is no significant difference between the numbers of spectra with $A > 0$ and $A < 0$. This quantifies the extent

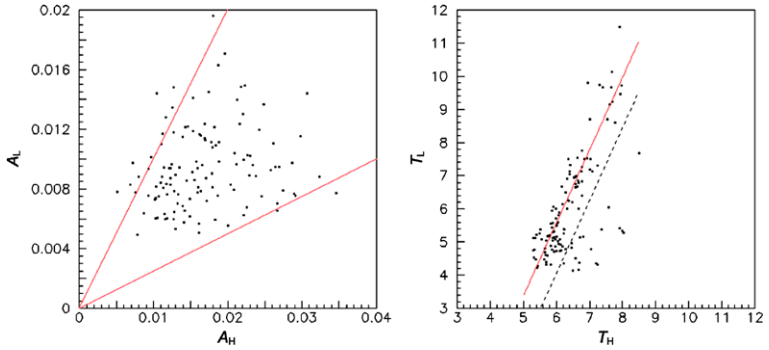

Figure 8 Distribution of category 2 intervals in the $(\langle A_L\rangle, \langle A_H\rangle)$ (left) and (T_L, T_H) (right) planes. Note that the ordinate and the abscissa scales differ by a factor of two on the left where the lines $\langle A_L\rangle = \langle A_H\rangle$ and $\langle A_L\rangle = 0.25\langle A_H\rangle$ have been drawn to guide the eye. On the right, the full line shows the best fit to family 1. The separation between the two families is indicated by a dashed line.

to which it is legitimate to ascribe a single period to each spectrum and, at the same time, shows that it is not a source of bias in our comparison between Learmonth and Ha Noi data.

In the remainder of the section, we restrict the analysis to family 1 and require, for both Learmonth and Ha Noi data, good quality fits to Equation (1) and large oscillation amplitudes ($\langle A_H\rangle > 1.0$ % and $\langle A_L\rangle > 0.6$ %). A plot of the values defined by

$$\alpha(t) = A(t)\sin(2\pi t/T + \varphi)/\big\langle A(t)\big\rangle \tag{6}$$

evaluated for the Ha Noi and Learmonth data reveals a positive phase correlation; it is illustrated in Figure 9 (left) by the dependence on $\alpha_L - \alpha_H$ of the correlation function C averaged over $\alpha_L + \alpha_H$. Here C is defined as

$$C = \frac{\mathrm{d}^2 N}{\mathrm{d}\alpha_L\,\mathrm{d}\alpha_H}\left[\frac{\mathrm{d}N}{\mathrm{d}\alpha_L}\right]^{-1}\left[\frac{\mathrm{d}N}{\mathrm{d}\alpha_H}\right]^{-1}. \tag{7}$$

The correlation is of the order of 15 %.

To reveal a possible correlation between the periods and amplitudes of the observed oscillations, we defined T^* and A^* as giving a measure of the periods and amplitudes averaged between Learmonth and Ha Noi:

$$T^* = \big\{(T_L - 6.3) + 2.2(T_H - 6.3)\big\}/3.2 \quad \text{and} \tag{8}$$

$$A^* = (A_H + 1.75A_L)/2.75. \tag{9}$$

Figure 9 (right panel) reveals a weak anti-correlation between these two quantities; all larger T^* intervals ($T^* > 0.6$ min) show lower amplitudes ($A^* < 1.1$ %).

Finally, to illustrate the average shape of the oscillations, Figure 10 displays the distribution of $[S(t) - P(t)]/A(t)$ over $\psi = 2\pi t/T + \varphi$ modulo(2π) for the Ha Noi and Learmonth data separately. Both show, on average, a clear sine wave.

4. Oscillations: Possible Instrumental Effects

As a check of the solar origin of the observed oscillations, we took data by pointing the telescope 15° off the Sun. The absence of observed oscillations allows placing an upper limit of

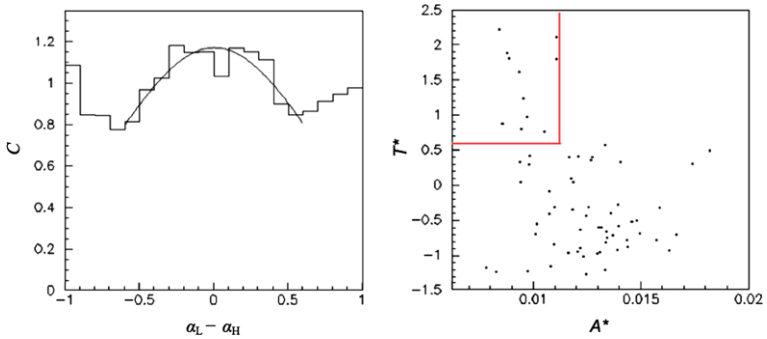

Figure 9 Left: phase correlation coefficient as a function of $\Delta\alpha = \alpha_L - \alpha_H$. Right: two-dimensional distribution in the (T^*, A^*) plane.

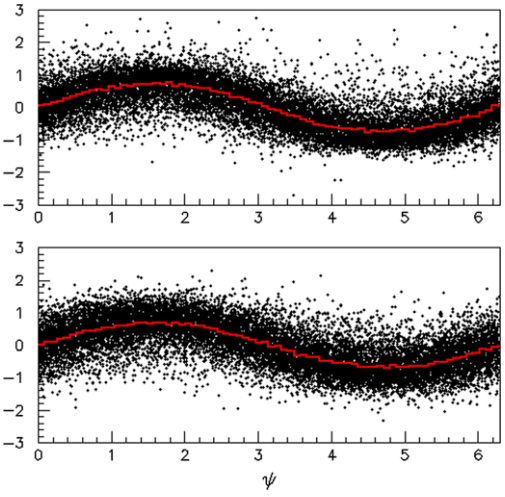

Figure 10 Shapes of the oscillations observed at Ha Noi (upper panel) and Learmonth (lower panel) as a function of ψ in radian. The lines indicate the average wave forms.

0.3 % on their possible relative amplitudes. Simple instrumental effects were excluded, such as resulting from electronics faults, *e.g.* saturation of electronics components. Generally, the evidence for a strong positive correlation between the periods of the oscillations observed at Ha Noi and Learmonth seems to exclude an interpretation in terms of simple instrumental effects. Nevertheless, the similarity between the two instruments implies that they suffer from similar biases or weaknesses, which might result in these positive correlations and in our misinterpretation of what they hide.

Such a possible source of erroneous interpretation was suggested to us by Dr. Owen Giersch (private communication, 2013) as arising from multipathing, that is, interferences between the direct solar signal and its reflection on a nearby obstacle (building, ground, *etc.*). Multipathing would indeed vary with the position of the Sun in the sky and result in different oscillation amplitudes and periods at Ha Noi and Learmonth because of their different local environment. For an obstacle at a distance D in a direction making an angle ω with respect to the Sun, the path difference is $D(1 - \cos\omega) \approx \frac{1}{2}D\omega^2$ as ω must be small enough for both the direct and reflected signals to be contained in the beam. Typically, $\omega \approx 0.1$ rad and $\mathrm{d}\omega/\mathrm{d}t \approx 3$ mrad min^{-1}. For the period $T = \lambda/(D\omega\,\mathrm{d}\omega/\mathrm{d}t)$ of typical multipath oscillations to be in the 6-min range, D therefore needs to be in a range of 100 m, which is a reasonable

value for possible nearby obstacles. Moreover, such oscillations would be observed for the time it takes the Sun to sweep across an angle of the order of the beam aperture, namely a fraction of an hour.

Multipathing therefore appears to be a serious candidate to account for in our observations. An important argument against it is the observation of the strong correlation between the periods of the oscillations measured at Learmonth and Ha Noi. A crucial test of the multipathing hypothesis would be the observation that it occurs preferentially when the Sun is low on the horizon. Splitting the distribution of elevations into three equally populated bins, 0° to 52°, 52° to 62°, and 62° to 90°, the fractions of category 2 intervals are 31 ± 6 %, 64 ± 8 %, and 24 ± 5 %. While this clearly excludes an excess of low-elevation occurrences as would be expected from multipathing involving obstacles on ground, it displays a significant excess at elevations of the order of 60°, by four standard deviations, for which we have no explanation. The combination of multipathing and spill-over into the antenna side-lobes could in principle generate oscillations at high elevations, but we cannot think of a sensible explanation along such lines.

5. Oscillations: Possible Physics Interpretations

To the extent that instrumental effects can be rejected, differences between the precise characteristics of the oscillations simultaneously observed at Learmonth and Ha Noi are intriguing and call for an explanation. Two possibilities come to mind as natural candidates: one is the effect of the different polarization states detected at Ha Noi and Learmonth. The other is the effect of different distortions in radio signals caused by their propagation through the local ionosphere. Indeed, the particular position of Ha Noi with respect to the geomagnetic equator implies a high ionospheric scintillation index S4,[4] as shown in Figure 11. There exists an abundant literature on the effects of scintillation on the L-band (1 – 2 GHz) transmission through the ionosphere (Smith and Flock, 1993; Basu *et al.*, 2002), providing evidence for major disturbances that affect both the amplitude and phase of the transmitted signals, with important dependences on solar activity and on time, both seasonal and diurnal, multipathing resulting from inhomogeneities of the local ionosphere.

Some of the features observed and reported here are reminiscent of the properties of coronal oscillations that have been studied extensively at visible and ultraviolet wavelengths (Roberts, 2000; Chen and Schuck, 2007). In particular, transverse oscillations in coronal loops have been identified by Aschwanden *et al.* (1999) using the *Transition Region and Coronal Explorer* (TRACE) in the extreme UV. They have periods of about 5 min, similar to those of photospheric oscillations, but are quickly damped. They have been interpreted as global oscillations, the loop being bodily displaced with the footpoints remaining fixed (kink mode), triggered by a flare shock. These oscillations have since been the target of new observations and have triggered the elaboration of several MHD models that aim to describe them. However, reports of these oscillations at radio wavelengths are much less common. Strong oscillations with a period of 5.6 min were once reported at 22 GHz (Strauss, Kaufmann, and Opher, 1980) as lasting for about 2 h using the Itapetinga radio telescope to track an active region of the Sun. Oscillations with periods ranging from 3 min to hours have been reported to be associated with solar active regions and are now extensively studied

[4]Australian Government, Bureau of Meteorology, Radio and Space Weather Services, http://www.ips.gov.au/Satellite/6/3.

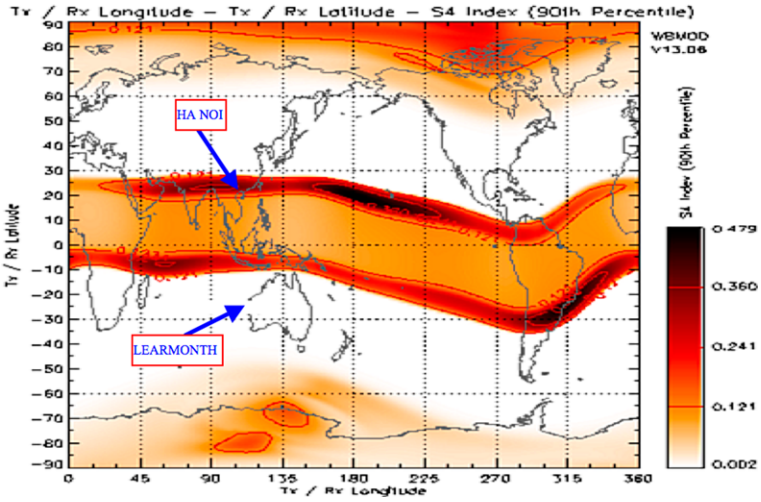

Figure 11 Typical geographical distribution of the ionospheric scintillation S4 index (http://www.ips.gov.au/Satellite/6/3).

using the Nobeyama Radioheliograph (Gelfreikh *et al.*, 2004). There have also been reports of an association of type II radio bursts, occurring from a few hundred MHz down to 1 MHz, with coronal loop oscillations (Hudson and Warmuth, 2004), but this does not seem to be related with what we observe.

While polarization effects are expected to be important in interpreting MHD oscillations, the Ha Noi and Learmonth data are not independent; the latter are a linear combination of the right-handed signals observed at Ha Noi with a left-handed component. It would be very instructive to compare observations made of the circularly polarized component at Ha Noi and Learmonth, either of the same or opposite handedness.

6. Summary

We observed the Sun using the VATLY radio telescope situated in Ha Noi at a frequency of 1415 MHz between mid-April and early September in 2012. The data were analysed together with similar data collected by the Learmonth Solar Observatory in Australia. Both sets of data show the same general features, including flares, of which three in early July were particularly strong. Comparison between the Learmonth and Ha Noi data shows that the former has lower noise by a factor of about 1.7, but provides evidence for the proper performance of the VATLY radio telescope.

The two sets of data display frequent oscillations at the percent level and with periods around 6 min that typically last for a fraction of an hour. We compared the properties of these oscillations in detail. The possibility that they might result from instrumental effects was explored. A particularly serious candidate for such an explanation is multipathing of radio signals, which, however, would not cause the strong observed correlation between Ha Noi and Learmonth periods. Moreover, in its simple form of being the result of reflections from obstacles on ground, it can be rejected as not being enhanced near the horizon. However, it illustrates how instrumental effects that we did not think about might possibly produce the observed oscillations. In particular, its most frequent occurrence at elevations close to 60°

remains unexplained. This caveat must be kept in mind when exploring possible physics interpretations.

While their amplitudes are uncorrelated, the oscillations observed at Ha Noi and Learmonth reach their higher periods as well as their lower periods at about the same times and tend to be in phase. However, when looked at time interval by time interval, they differ significantly, displaying important smearing with respect to this average behaviour. Moreover, the average amplitude observed at Ha Noi is larger than that at Learmonth by a factor of about 1.75, while the period span observed at Learmonth is longer than that at Ha Noi by a factor of about 2.2.

Two physical effects that might be relevant are different polarization states (circular at Ha Noi, linear at Learmonth) or multipath effects resulting from inhomogeneous ionospheric transmissions (Ha Noi sits on a maximum of the S4 scintillation index while Learmonth is normal).

Acknowledgements We are deeply indebted to the Learmonth Solar Observatory staff, who are making their data available to the public, and particularly to Dr. Owen Giersch for kindly answering many of our questions related to these data. Financial and/or material support from the Institute for Nuclear Science and Technology, Vietnam National Foundation for Science and Technology Development (NAFOSTED) under grant number 103.08-2012.34, the World Laboratory and Odon Vallet fellowships is gratefully acknowledged.

References

Aschwanden, M.J., Fletcher, L., Schrijver, C.J., Alexander, D.: 1999, *Astrophys. J.* **520**, 880.

Basu, S., Groves, K.M, Basu, S., Sultan, P.J.: 2002, *J. Atmos. Solar-Terr. Phys.* **64**, 1745.

Chen, J., Schuck, P.W.: 2007, *Solar Phys.* **246**, 145.

Gelfreikh, G.B., Shibasaki, K., Nagovitsyna, E.Yu., Nagovitsyn, Yu.A.: 2004. In: Stepanov, A.V., Benevolenskaya, E.E., Kosovichev, A.G. (eds.) *Multi-wavelength Investigations of Solar Activity*, *IAU Symp.* **223**, 245.

Hiep, N.V.: 2012, Observation of the 21 cm sky using the VATLY radio telescope, M.S. thesis, Ha Noi Institute of Physics.

Hiep, N.V., Anh, P.T., Darriulat, P., Diep, P.N., Dong, P.N., Hoai, D.T., Nhung, P.T., Thao, N.T.: 2012, *Commun. Phys. Vietnam* **22**, 365.

Hiep, N.V., Anh, P.T., Darriulat, P., Diep, P.N., Dong, P.N., Hoai, D.T., Nhung, P.T., Thao, N.T.: 2013, *Commun. Phys. Vietnam* **23**, in press. http://www.inst.gov.vn/Vatly/publications.htm.

Hudson, H.S., Warmuth, A.: 2004, *Astrophys. J.* **614**, 85.

Roberts, B.: 2000, *Solar Phys.* **193**, 139.

Smith, E.K., Flock, W.L.: 1993, In: Davarian, F. (ed.) *Proceedings of the Seventeenth NASA Propagation Experimenters Meeting and the Advanced Communications Technology Satellite Propagation Studies Miniworkshop, NASA CR-194096*, 203.

Strauss, F.M., Kaufmann, P., Opher, R.: 1980, *Solar Phys.* **67**, 83.